THE JOURNAL OF PHYSICAL CHEMISTRY B

ARTICLE

pubs.acs.org/JPCB

Ligand Exchange Reaction Involving Ru(III) Compounds in Aqueous Solution: A Hybrid Quantum Mechanical/Effective Fragment Potential Study

Charles M. Aguilar and Willian R. Rocha*

Departamento de Química, ICEX, Universidade Federal de Minas Gerais 31270-901, Pampulha, Belo Horizonte, MG, Brazil

Supporting Information

ABSTRACT: In this work, the hybrid density functional theory/effective fragment potential (DFT/EFP) approach was applied to investigate the ligand exchange reactions $[Ru(NH_3)_4(Cl)(\mathbf{L})]^{2+}(aq) + H_2O \rightarrow [Ru(NH_3)_4(H_2O)(\mathbf{L})]^{3+}(aq) + Cl^-(aq)$ in solution, with **L**= NH_3 and pyridine (Py). A procedure to generate the EFP water clusters is described. The reaction proceeds through an interchange mechanism with dissociative character, I_d, and displays a high sensitivity to the basicity of the ligand trans to the chloride. Changing the nature of the nitrogenated ligand has a drastic impact on the activation and reaction energy. When ammonia is used, the activation energy, computed at the B3LYP/cc-pVDZ/EFP level of theory is 22.7 kcal/mol, which is ~40% higher than the value of 13.4 kcal/mol computed when for **L** = Py. In addition, the spontaneity of the reaction changes upon changing the nature of the nitrogenated ligand. Changing the level of theory used in the QM part of the calculation from B3LYP/cc-PVDZ to MP2/cc-pVTZ does not change the results appreciably, and inclusion of long-range effects by means of the polarizable continuum model has a negligible effect on the energetic of the reaction. The activation enthalpy computed at the B3LYP/cc-pVDZ/EFP is in very good agreement with the experimental findings, attesting to the validity of the QM/EFP approach used in this work.

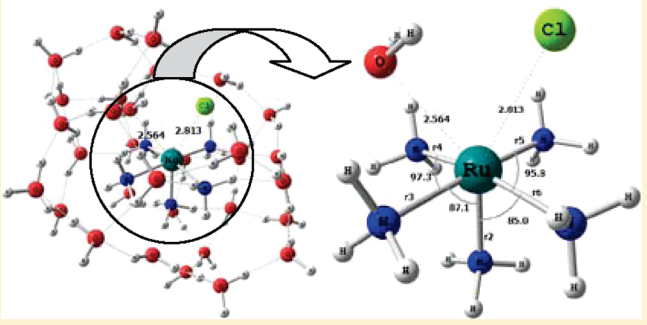

INTRODUCTION

Ruthenium compounds with amine ligands have a vast range of applications in important biochemical and pharmacological processes.[1] To cite a few applications, they have been used as antitumor agents,[2] in radiotherapy,[3] in photodynamic therapy,[4] immunosuppressive agents,[5] and as compounds involved in the controlled released of nitric oxide.[6] In their common oxidation states, these ruthenium compounds show octahedral structures in solution, which are relatively inert to ligand exchange reactions. Therefore, it is believed that the antitumor action mechanism of the Ru(II) and Ru(III) compounds is probably different from the mechanism observed for the antitumor compounds of Pt(II), which are square−planar and act through crossing bonds to the DNA.[7] The antitumor activity of Ru(II)/Ru(III) compounds is based on the hypothesis of activation by reduction,[8] which suggests that the Ru(III) compounds act as pro-drugs that are activated by reduction in vivo, facilitating their coordination to the target biomolecules.

Ruthenium compounds of the type $[Ru(Cl)(NH_3)_5]^{2+}$, *trans*-$[Ru(Cl)(NH_3)_4(pyridine)]^{2+}$, [IndH]*trans*-$[Ru(Cl)_4(indazole)_2]$ (Ind = indazole), and [Im]*trans*-$[Ru(Cl)_4(DMSO)(imidazole)]$ (Im = imidazole), known as NAMI-A, are active against some kinds of cancer.[9−12] To reach its biological targets inside the cell this compound is activated through a ligand exchange reaction involving a chloride ligand and a water molecule in solution, as shown in Scheme 1.

Ligand exchange reactions are one of the most important processes occurring with inorganic or organometallic complexes in solution and have been the subject of extensive reviews.[13−17] For octahedral complexes, there are three possible mechanisms,[18] which are summarized in Figure 1.

The associative mechanism passes through a transition state to form a reactive intermediate in which the coordination number of the transition metal center is increased by 1. The dissociative mechanism takes place through a transition state leading to an intermediate with lower coordination number. Between these two extreme mechanisms, there are the interchange mechanisms, characterized by a synchronous movement between the incoming and leaving ligands. Depending on the contribution of the entering and leaving ligands to the transition state, these interchange mechanisms are classified as associative interchange (I_a), in which bond-making is more important; interchange (I), in which both bond-making and bond-breaking are of similar importance; and the dissociative interchange (I_d), in which the

Received: October 25, 2010
Revised: December 15, 2010
Published: February 15, 2011

Scheme 1

$$[Ru(NH_3)_4(\mathbf{L})(Cl)]^{2+}(aq.) + H_2O \longrightarrow [Ru(NH_3)_4(\mathbf{L})(H_2O)]^{3+}(aq.) + Cl^-(aq.)$$

$$ML_nX \longrightarrow ML_n + X \xrightarrow{Y} ML_nY \qquad (D)$$

$$ML_nX + Y \longrightarrow ML_nXY \longrightarrow ML_nY + X \qquad (A)$$

$$ML_nX + Y \longrightarrow X\cdots\cdots ML_n \cdots\cdots Y \longrightarrow ML_nY + X \qquad (I)$$

Figure 1. Possible mechanism involved in the ligand exchange reactions in octahedral compounds: (A) associative mechanism, (D) dissociative mechanism and (I) interchange mechanism.

bond breaking contributes more. For octahedral Ru(III) complexes, such as those studied in this work, it is well accepted, on the basis of theoretical and experimental results, that the reaction takes place according to a interchange mechanism with associative or dissociative character (I_a or I_d).[13] In fact, as we shall see, this was the main reaction pathway investigated in this work.

The theoretical modeling of this ligand exchange process involving transition metal complexes in solution is a challenging task. One commonly used procedure would involve the study of the reaction mechanism in gas phase and then, using thermodynamics cycles, estimating the reaction energetic in solution. However, this procedure turns out to be difficult for transition metal complexes, since some of the species involved along the reaction coordinate exist only in solution. For instance, if we try to optimize the structure of the transition state structures involved in the mechanisms, shown in Figure 1, in the gas phase, the species dissociates spontaneously. This means that the solvent effects must be included already in the geometry optimization step. Classical methods based on nonreactive empirical force fields are not adequate to treat these processes involving bond-breaking/-making, and depending on the transition metal of interest, there will be the necessity of parametrizing these force fields, which is not an easy task. However, these MM methods can be used to describe the solvent molecules in combined QM/MM schemes.[19,20]

Two other important aspects impose several difficulties in the treatment of transition metal compounds in solution: (i) the correct description of the interaction of the transition metal compounds, in their ground electronic state, with the solvent, which is essential to generate the liquid structure around the complex; and (ii) the solvent effects on the stability of different spin multiplicities of a partially filled d shell, which requires an adequate quantum mechanical method to describe these electronic states. In recent years, however, much progress has been achieved to deal with reactive processes involving transition metal ions/compounds in solution, in particular, the use of QM/MM simulation protocols[21] and the Car−Parrinello density functional molecular dynamics method,[22,23] which have shed some light on this complex problem. Another important approach to study transition metal compounds in solution, particularly if the main interest is in spectroscopy, is the sequential QM/MM (S-QM/MM) developed by Canuto and Coutinho.[24,25]

Despite the aforementioned problems, several theoretical studies have been conducted to investigate the hydrolysis processes of platinum and ruthenium antitumor complexes.[23,26,27] For the case of ruthenium complexes, the studies have been focused on the promising antitumor compounds NAMI-A[27b,27c] and ICR.[27a] Chen et al.[27b] studied the hydrolysis process of the NAMI-A complex at the DFT level of theory using the hybrid B3LYP exchange-correlation functional,[36,37] including the solvent effects with the CPCM continuum salvation model. An activation free energy of 23.2 kcal/mol was found, which is in satisfactory agreement with the experimental results. However, the results obtained for the second hydrolysis step, which was attributed to the solvent model used, were in disagreement with the experimental findings.

Bešker et al.[27c] also studied the same hydrolysis processes of NAMI-A, using the same hybrid exchange-correlation functional and modeling the solvent effects with the Poisson−Boltzmann continuum solvation method and including three water molecules explicitly. The authors found good agreement between the calculated and experimental activation enthalpy for the first and second hydrolysis step. These two independent studies on NAMI-A have found a dissociative interchange mechanism, I_d, for the chloride/water ligand exchange reaction and the activation free energies computed for the first hydrolysis process around 24 kcal/mol. Chen et al.[27a] has also investigated the hydrolysis processes for the ICR complex using the same formalism used for the NAMI-A complex. The authors have found good agreement with the experimental results for the activation free energies involved in the first and second hydrolysis steps.

In this work, we studied the energies and mechanisms involved in the chloride/water exchange reaction in the compounds $[Ru(NH_3)_4(Cl)(\mathbf{L})]^{2+}$ ($\mathbf{L}$ = NH_3 and pyridine (Py)) in aqueous solution, as shown in Scheme 1. In contrast with the NAMI-A and ICR complexes, these compounds have only one hydrolyzable chloride ligand, which allows a systematic study focusing only on this chloride/water exchange process. Thus, one of the main goals of this work is to investigate the effect of different nitrogen ligands on the kinetics and mechanism of the reaction. The hybrid quantum mechanical/effective fragment potential (QM/EFP) approach developed by Gordon and co-workers[28−30] was used to include solvent effects on the structures and reaction energies along the entire potential energy surface describing the reaction. As we shall see, the QM/EFP is an efficient method in describing these ligand exchange processes in aqueous solution, which proceeds via the I_d mechanism and shows a high sensitivity to the nature of the amine ligand displaced.

COMPUTATIONAL DETAILS

The EFP method of Gordon and co-workers was originally formulated to describe chemical reactions in solution[30,31] and has been successfully applied to study reactions in aqueous solutions.[31−35] In this method, the system is partitioned into a reactive or quantum mechanical region composed of the solute, and the solvent molecules are treated explicitly as fragments (EFPs), described as a set of one electron potentials (V) that are added to the Hamiltonian of the quantum mechanical region. The Hamiltonian of the entire system is then described as

$$H_{total} = H_{QM} + V \qquad (1)$$

The potential, V, contains terms describing (i) Coulombic interactions between solvent molecules and solvent molecules with the QM solute, including charge penetration; (ii) polarization or induction interaction between solvent molecules and

solvent molecules with the QM solute; and (iii) exchange repulsion, charge transfer, and other terms that are not taken into account in the previous two terms. The first two terms are determined entirely by QM calculations on a single solvent molecule, and the third term is fitted to the QM water dimer potential. In this work, we used the DFT-based EFP1 method[28] in which the potential V is obtained at the DFT level by using the B3LYP exchange-correlation functional.[36,37] The detailed description of the potentials used to describe these interactions, how they can be obtained, and how the method is implemented is very well documented in several elegant articles from Gordon and co-workers.[28−32] The QM/EFP method has the very attractive characteristic of not needing intermolecular parametrizations involving the solute, which is particularly important to deal with reactions involving transition metal compounds in solution, for which there is a lack of available intermolecular interaction potentials.[38,39] Additionally, the availability of analytical gradients and numerical Hessian makes it possible to optimize the transition state structures and follow the intrinsic reaction coordinate for the reaction in the presence of the EFP's solvent molecules.

In a recent work,[40] we developed a protocol to generate the large clusters of EFP's water molecules to be used in the QM/EFP approach. First, a suitable guessed transition state structure was constructed and an initial classical Monte Carlo (MC) simulation[41,42] is performed, keeping this initial transition state structure frozen. This structure was submitted to a single point calculation at the B3LYP level by using the LANL2DZ[43] effective core potential and its associated double-ξ valence basis functions for the Ru and 6-31+G(d) basis set[44] for other atoms, just to obtain an initial charge distribution on the atoms using the charges derived from the electrostatic potentials method.[45] In all QM calculations, the ruthenium atom was treated in its low spin state configuration (S = 1/2), since previous test calculations showed that the complexes with ruthenium in its high spin configuration (S = 5/2), when obtained, are much higher in energy. The Lennard-Jones (LJ) intermolecular potentials parameters, used for the transition state (TS) guess structure, were taken from the optimized potentials for liqid simulations (OPLS) force field,[46] and the Ru^{3+} parameters were taken from the universal force field (UFF) force field.[47] The water molecules were frozen in their EFP1/DFT geometry (O−H bond distance of 0.9468 Å and H−O−H angle of 106.70°),[28] and the σ and ε parameters of the LJ potential were obtained from the TIP3P[48] water model. The system consisted of one solute molecule (the TS guess structure) and 600 water molecules. A small MC simulation of 6.0 × 10^6 MC steps was conducted, and the analysis of the radial pair distribution function between the center-of-mass of the TS structure and the center-of-mass of the EFP water, $g_{cm\text{-}cm}(r)$, showed ∼30 EFP water molecules distant up to 7 Å from the solute molecule, as shown in Figure 2. One configuration containing the nearest 30 water molecules was arbitrarily selected, and then this cluster (transition state guess plus 30 water molecules) was used was the additional steps. The initial structure of these clusters is shown in Figure S1 of the Supporting Information material. It is noteworthy that this initial MC simulation is conducted only to build up the initial EFP water cluster around the TS guessed structure, and this justifies the use of approximate intermolecular parameters. These clusters, as described below, will be subject to a global optimization process to find the optimal arrangement of the EFP molecules around the solute molecule within the B3LYP/EFP potential

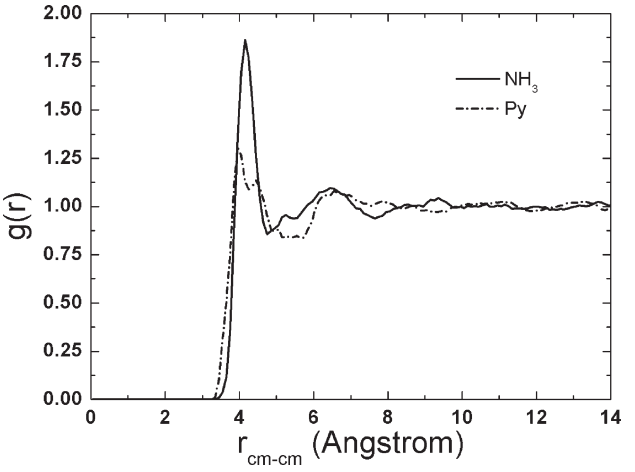

Figure 2. Radial pair distribution function between the center-of-mass of the TS guess structure and the center-of-mass of the EFP water.

energy surface. The advantage of this approach in constructing the initial EFP water cluster is that the EFP fragments come from a previously selected, Boltzmann-weighted configuration.

The initial EFP cluster obtained in the MC simulation was then submitted to a global optimization[49] at 300 K. In this procedure, all the internal coordinates of the guess transition state structure were kept frozen, while the EFP water molecules moved in a cubic box of 10 Å on each side. Using this procedure, we can select the lowest-energy configuration of the EFP molecules around the frozen transition state structure. It is noteworthy that the convergence criterion of the gradient for this rotation and translation of the EFP water molecules should be very low because this is a very flat potential energy surface and we used a criterion of 10^{-5} for the maximum gradient. With this lowest energy cluster arrangement, we performed a full geometry optimization of the transition state in the presence of the EFP water molecules at the B3LYP level of theory using the DZVP[50] for the Ru and cc-pVDZ[51] basis set for the other atoms, followed by frequency calculation at the same level to verify the nature of the stationary points located on the potential energy surface and also to include zero point energy (ZPE) corrections on the energies obtained and thermal corrections to the Gibbs free energy at room temperature. To obtain a deeper insight into the reaction mechanism, in solution, we calculated the intrinsic reaction coordinate (IRC)[52] by using the Gonzalez−Schlegel second-order path,[53,54] starting from the optimized transition-state structure, with a step length of 0.30 $(amu)^{1/2}$ Bohr. In addition, single-point calculations at the second-order Møller−Plesset (MP2) level,[55,56] using the cc-pVTZ[57,58] basis set, were carried out at the stationary points located along the IRC. The initial EFP water cluster was generated using the DICE program of Canuto and Coutinho,[59] and all other calculations were performed with the GAMESS (US) program.[60]

RESULTS AND DISCUSSION

Structural Results. The optimized structures of the transition states involved in the chloride/water exchange reactions of Scheme 1, inside the EFP water clusters, are shown in Figures 3 and 4. Both structures exhibit an increased coordination number around the ruthenium atom, with a loose bonding of the chloride and water ligands. The structures are stabilized by hydrogen

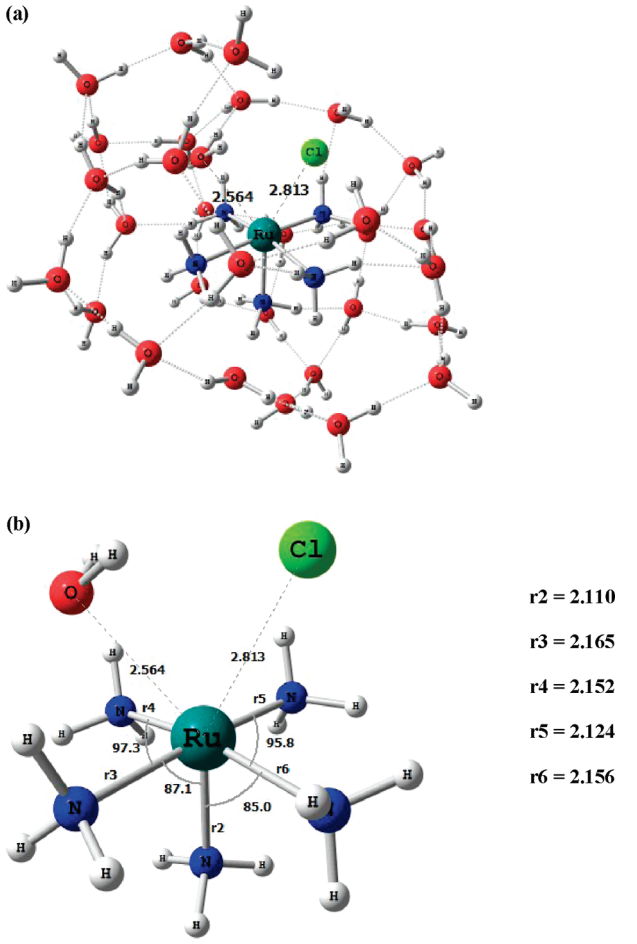

Figure 3. Optimized structure for the transition state (TS) involved in the chloride/water exchange in the compound $[Ru(NH_3)_4(Cl)(NH_3)]^{2+}$. Top: TS plus 30 EFP water molecules. Bottom: TS species with the EFP fragments removed for clarity. Distances are reported in angstroms; angles, in degrees.

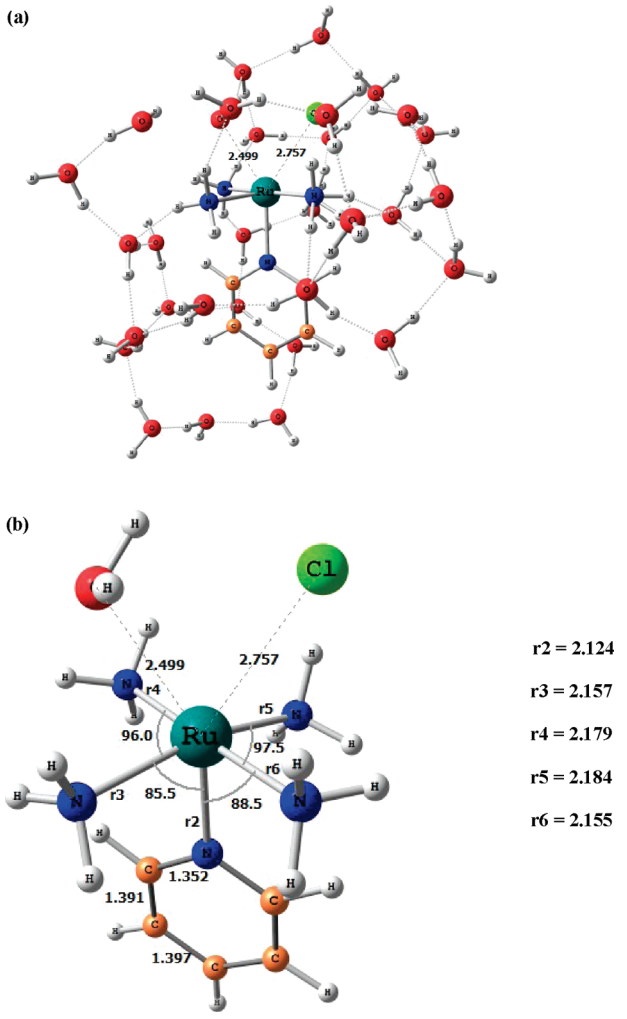

Figure 4. Optimized structure for the transition state (TS) involved in the chloride/water exchange in the compound $[Ru(NH_3)_4(Cl)(Py)]^{2+}$. Top: TS plus 30 EFP water molecules. Bottom: TS species with the EFP fragments removed for clarity. Distances are reported in angstroms; angles, in degrees.

bonds with the EFP fragments, and this is crucial to obtain it; otherwise, without the EFP fragments, these structures tend to dissociate. The structures were characterized as first-order transition state by having imaginary frequencies of 94.3i (**L** = NH_3) and 95.7i cm^{-1} (**L** = Py). Analysis of the nuclear displacements associated with these imaginary modes shows a concerted motion involving the incoming water molecule and the leaving chloride ligand, which is consistent with an interchange mechanism in which the incoming and leaving ligands are exchanged in a single step. In both structures, the entering and leaving ligands make an angle of 66°. It is noteworthy that when **L** = Py, the distances involved in the reactive region of the TS structures are all small when compared with the values when **L** = NH_3. For instance, for **L** = Py, the Ru−Cl and Ru−H_2O distances are 2.757 and 2.499 Å, respectively, which are 0.056 and 0.065 Å smaller than the values obtained for **L** = NH_3 for this same distances.

For a deeper insight into the exchange mechanism in solution, we carried out the IRC calculations, which determine the steepest descent path from the transition state connecting reactants and products. The variation of the main structural parameters along the IRC for both complexes is shown in Figure S2, and the optimized structures of reactants and products obtained along the IRC for the exchange mechanism, inside the EFP cluster, for the complex $[Ru(NH_3)_4(Cl)(NH_3)]^{2+}$ are shown in Figures 5 and 6, and for the complex $[Ru(NH_3)_4(Cl)(Py)]^{2+}$, in Figures S3 and S4. The variation in the Ru−Cl and Ru−H_2O distances along the IRC follows the same profile for the two complexes studied. For the complex $[Ru(NH_3)_4(Cl)(Py)]^{2+}$, the initial Ru−$H_2O$ distance is 3.785 Å (S = −23.5), with the value of 2.499 Å at the transition state (S = 0.00) and then reduction to 2.082 Å at the product (S = 23.5). At the same time, the Ru−Cl distance increases from 2.392 to 2.757 Å (S = 0.00) and continues to increase to 4.038 Å at the product.

As can be seen in Figures 6 and S4, the products for both reactions display a distorted octahedral structure, with the incoming ligand occupying the axial position. Comparing the Ru−Cl distances computed for the reactant and the transition state and also the Ru−H_2O distance in the product and in the transition state may give an indication if this interchange mechanism is associative or dissociative in nature. That is, if the Ru−Cl bond breaking or the Ru−H_2O bond making will be the most relevant for the product formation. The Ru−Cl distance computed for the reactant $[Ru(NH_3)_4(Cl)(NH_3)]^{2+}$

dx.doi.org/10.1021/jp110198h |J. Phys. Chem. B 2011, 115, 2030–2037

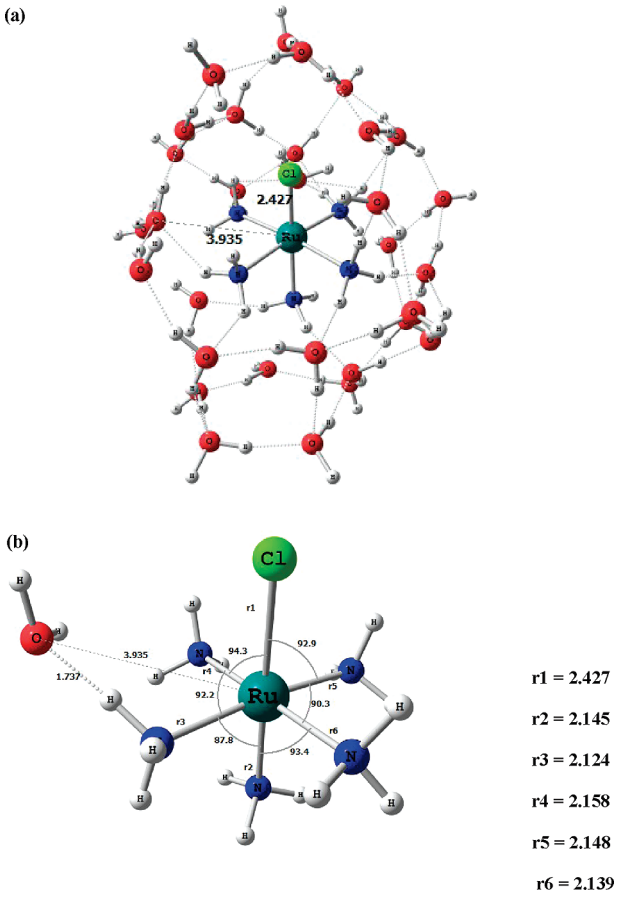

Figure 5. Optimized structure for the reactant species generated in the IRC for the chloride/water exchange in the compound $[Ru(NH_3)_4(Cl)(NH_3)]^{2+}$. Top: reactant plus 30 EFP water molecules. Bottom: reactant species with the EFP fragments removed for clarity. Distances are reported in angstoms; angles, in degrees.

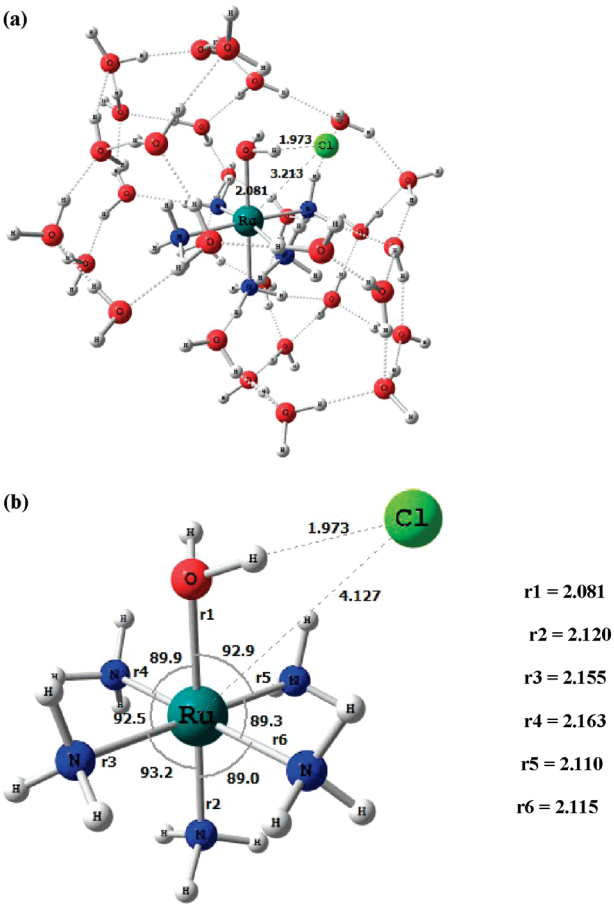

Figure 6. Optimized structure for the product species generated in the IRC for the chloride/water exchange in the compound $[Ru(NH_3)_4(Cl)(NH_3)]^{2+}$. Top: product plus 30 EFP water molecules. Bottom: product species with the EFP fragments removed for clarity. Distances are reported in angstroms; angles, in degrees.

species (2.427 Å, Figure 7) is 16% elongated at the transition state (2.813 Å, Figure 4). However, the Ru−H_2O distance at the transition state (2.564 Å) is 23% elongated when compared with the Ru−H_2O distance of 2.081 Å in the product $[Ru(NH_3)_4(H_2O)(NH_3)]^{2+}$, Figure 6. These results indicate that the Ru−Cl bond is more tightly bonded at the transition state than the Ru−H_2O, so the Ru−Cl bond will be more difficult to break than the formation of the Ru−H_2O bond in the product species, indicating that this interchange mechanism may be classified as dissociative, I_d.

When the $[Ru(NH_3)_4(Cl)(Py)]^{2+}$ is used, the same reasoning applies. As can be seen in Figures S3, 4 and S4, the Ru−Cl bond at the transition state is 15% elongated, and the Ru−H_2O bond is 20%, also indicating an I_d type of mechanism, with the Ru−Cl bond-breaking being determinant.

Energetic Results. The QM/EFP energies variation along the reaction coordinate for the chloride/water exchange reactions are shown in Figure 7, and the results for the stationary points are quoted in Table 1. The energetic results show that this ligand exchange reaction is very sensitive to the nature of the nitrogen ligand **L** trans to the chloride in the complexes $[Ru(NH_3)_4(Cl)(\mathbf{L})]^{2+}$. At the B3LYP/cc-pVDZ/EFP level of theory, the reaction proceeds with an activation energy of 22.7 kcal/mol, when **L** = NH_3, which is ∼40% higher than the value of 13.4 kcal/mol computed when for **L** = Py. Furthermore, the reaction is endothermic, with a reaction energy 2.3 kcal/mol, when **L** = NH_3 and proceeds exothermically, with a reaction enthalpy of −21.2 kcal/mol for **L** = Py. Treating the QM system at the MP2 level, with a larger basis set, MP2/cc-pVTZ, has small effect on the activation energies and also on the reaction energy, except for **L** = NH_3, in which the reaction energy changes from 2.3 to 5.0 kcal/mol at the MP2/cc-pVTZ/EFP level of theory.

To analyze the effects of long-range electrostatic interactions on the EFP water cluster, we performed single-point calculations on the optimized structures by using the polarizable continuum solvation model (PCM),[61,62] at the B3LYP/cc-PVDZ level, with the molecular cavity being generated with the GEPOL-GB method.[63] The B3LYP/cc-PVDZ/EFP/PCM results quoted in Table 1, show that inclusion of long-range solvent effects with PCM has a negligible effect on activation and reaction energies computed for both compounds, which suggests that the large EFP cluster used is already capturing the important local and long-range effects.

Table 2 shows the enthalpy and Gibbs free energy variation for the chloride/water exchange computed at the B3LYP/cc-pVDZ/EFP level of theory. The thermal corrections (ΔG_T and ΔH_T) to the relative electronic−nuclear energy values ($\Delta E_{elect\text{-}nucl.}$) were computed from frequency calculations carried out at 25 °C. The activation enthalpy of 23.7 kcal/mol computed for the chloride/

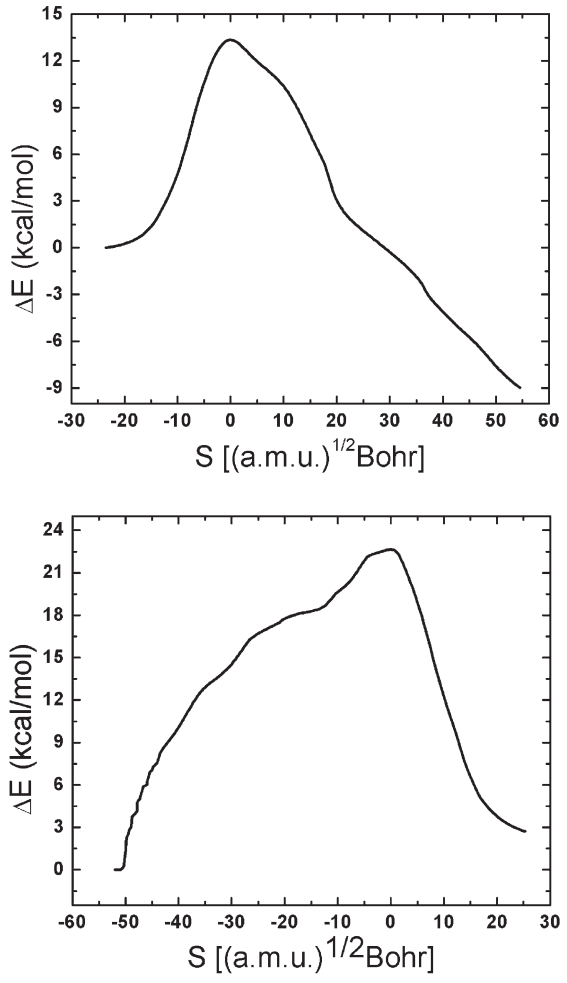

Figure 7. Intrinsic reaction coordinate (IRC) for the chloride/water exchange in the compounds $[Ru(NH_3)_4(Cl)(NH_3)]^{2+}$ (top) and $[Ru(NH_3)_4(Cl)(Py)]^{2+}$ (bottom).

Table 1. QM/EFP Calculated Relative Energies, ΔE, for the Chloride/Water Exchange Reaction in the Complexes $[Ru(NH_3)_4(Cl)(L)]^{2+a}$

level of theory used in the QM part	reactant	transition state	product
		L = NH_3	
B3LYP/cc-pVDZ	0.0	22.7	2.3
MP2/cc-pVTZ[b]	0.0	23.0	5.0
B3LYP/cc-pVDZ/PCM[b]	0.0	23.8	4.3
		L = Py	
B3LYP/cc-pVDZ	0.0	13.4	−21.2
MP2/cc-pVTZ[b]	0.0	14.6	−20.4
B3LYP/cc-pVDZ/PCM[b]	0.0	13.8	−19.7

[a] The energy values reported include the ZPE corrections. [b] Single-point calculations on the B3LYP/cc-pVDZ/EFP optimized structure. Values are given in kcal mol^{-1}.

water exchange in the complex $[Ru(NH_3)_4(Cl)(NH_3)]^{2+}$ is in very good agreement with the experimental value of 23.2 kcal/mol,[64] which demonstrates the validity of the approach used in this work. The values computed for the Gibbs free energy also

Table 2. Relative Enthalpy, ΔH, and Gibbs Free Energies, ΔG, for the Chloride/Water Exchange Reaction in the Complexes $[Ru(NH_3)_4(Cl)(L)]^{2+a}$

property	reactant	transition state	product
		L = NH_3	
ΔH	0.0	23.7 (23.2)[c]	3.9
ΔG	0.0	27.6	6.6
		L = Py	
ΔH	0.0	14.2	−18.3
ΔG	0.0	14.7	−17.0

[a] Computed at the B3LYP/cc-pVDZ/EFP level of theory. [b] Values are given in kcal mol^{-1}. [c] Experimental value taken from ref 64.

shows that the reaction is spontaneous for Py, $\Delta G_{reac} = -17.0$ kcal/mol, and the exchange process is not spontaneous when NH_3 is used, $\Delta G_{reac} = 6.6$ kcal/mol. Using the activation free energy results computed for the chloride/water exchange, we can evaluate, within the transition state theory,[65,66] the exchange (or in this case, hydrolysis) rate constant using eq 2:

$$k = \frac{k_B T}{h} e^{-\Delta G/RT} \quad (2)$$

where k_B is the Boltzmann's constant, T is the temperature (298.15K), R is the universal gas constant, h is the Planck's constant, and $\Delta G^{\#}$ is the Gibbs free energy of activation for the reaction. Using the QM/EFP values computed for the Gibbs free energy of activation, shown in Table 2, in eq 2, we obtain the values of $k = 4.1 \times 10^{-8}$ s^{-1} for the hydrolysis rate constant when NH_3 is used and $k = 111.2$ s^{-1} when the ligand is Py. Our hydrolysis rate constant computed for the NH_3 ligand is in line with the experimental result of 3.1×10^{-6} s^{-1}.[64] The high hydrolysis rate constant for the ligand Py can be attributed to the increase in the electron density on the metallic center, as compared with NH_3. This then leads to a weakening of the Ru−Cl bond trans to it, favoring the reaction to take place with a lower activation energy and increasing the rate for the hydrolysis process. Once the Ru(III) aqua complex is formed, it is reduced inside the cell to the complex *trans*-$[Ru(H_2O)(Py)(NH_3)_4]^{2+}$, in which the ruthenium atom is in the 2+ formal oxidation state. Experimentally, it is observed that this complex has a high affinity to bind the N7 site of the guanine base of the DNA,[1] in contrast to the NH_3 analog *trans*-$[Ru(H_2O)(NH_3)_5]^{2+}$ which is less selective and can bind to the guanine, cytosine, and adenine bases.[1,67] However, the binding kinetics of the compound *trans*-$[Ru(H_2O)(Py)(NH_3)_4]^{2+}$ to the DNA is slow, which is compensated by the high hydrolysis constant of the Ru(III) compound *trans*-$[Ru(Cl)(Py)(NH_3)_4]^{2+}$, increasing the biodisponibility of the Ru(III)−Py−aqua complex inside the cell.[1,67] Therefore, our results are in line with the experimental observations.

CONCLUSION

In this work, we investigated the ligand exchange reactions $[Ru(NH_3)_4(Cl)(\mathbf{L})]^{2+}(aq) + H_2O \rightarrow [Ru(NH_3)_4(H_2O)(\mathbf{L})]^{2+}(aq) + Cl^-(aq)$ in solution, with **L** = NH_3 and pyridine. The hybrid QM/EFP approach was used to include the solvent effects on structures and reaction energetic along the entire potential energy surface of the reactions. The systems

under study consisted of one solute molecule, treated at the B3LYP/cc-pVDZ level of theory surrounded by 30 EFP water molecules, selected using a new strategy to build the initial EFP cluster, by running a classical Monte Carlo simulation and analyzing the center-of-mass radial pair distribution function.

The results indicate that the reaction proceeds through an interchange mechanism with dissociative character, I_d, with the Ru−Cl bond cleavage being more important for the product formation. The reaction is very sensitive to the basicity of the ligand. Changing the nature of the amine ligand has a drastic impact on the activation and reaction energy. For instance, when ammonia is used, the enthalpy of activation, computed at the B3LYP/cc-pVDZ/EFP level, is 23.7 kcal/mol; however, when pyridine is used, the activation enthalpy is reduced ∼40%, assuming the value of 14.2 kcal/mol. The computed B3LYP/cc-pVDZ/EFP activation enthalpies are in very good agreement with the experimental findings. The inclusion of long-range solvent effects with PCM does not alter significantly the activation and reaction energies, which indicates that the large EFP water cluster used is capturing most of the important solvent effects. The computed rate constants for the hydrolysis process shows that when pyridine is used, the reaction occurs much faster ($k = 111.2\ s^{-1}$) than when ammonia is used ($k = 4.1 \times 10^{-8}\ s^{-1}$). The high hydrolysis rate constant for the ligand Py can be attributed to the increase in the electron density on the metallic center, as compared with NH_3. This then leads to a weakening of the Ru−Cl bond trans to it, favoring the reaction to take place with a lower activation energy and increasing the rate for the hydrolysis process. The agreements found with the experimental results validates the QM/EFP approach used here to study the ligand exchange reactions, and we are currently using this approach to study other chemical reactions in solution and also to investigate solvent effects on spectroscopic properties.

■ ASSOCIATED CONTENT

Supporting Information. Figures S1−S4, cited in the text, and the B3LYP/cc-pVDZ/EFP optimized structures (in Cartesian coordinates) of the transition state, reactants and products. This material is available free of charge via the Internet at http://pubs.acs.org.

■ AUTHOR INFORMATION

Corresponding Author

*Fax: +55 31 34095700. E-mail: wrocha@ufmg.br.

■ ACKNOWLEDGMENT

The authors thank the CNPq (Conselho Nacional de Desenvolvimento Científico e Tecnológico, INCT-Catálise) and FAPEMIG (Fundação de Amparo à Pesquisa do Estado de Minas Gerais) for financial support and research grants. C.M.A also thanks the CNPq for the scholarship grant.

■ REFERENCES

(1) Clarke, M. J. *Coord. Chem. Rev.* **2002**, *69*, 232.
(2) Mestroni, G.; Alessio, E.; Sava, G.; Pacor, S.; Coluccia, M.; Boccarelli, A. *Metal Based Drugs* **1994**, *1*, 41.
(3) Möller, T. R.; Ceberg, J.; Einhorn, N.; Lindholm, C.; Nylén, U.; Svensson, H. *Acta Oncol.* **2003**, *42*, 376.
(4) Schmitt, F.; Govindaswamy, P.; Süss-Fink, G.; Ang, W. H.; Dyson, P. J.; Juillerat-Jeanneret, L.; Therrien, B. *J. Med. Chem.* **2008**, *51*, 1811.
(5) Bastos, C. M.; Gordon, K. A.; Ocain, T. D. *Bioorg. Med. Chem. Lett.* **1998**, *8*, 147.
(6) Pieper, G. M.; Roza, A. M.; Adams, M. B.; Hilton, G.; Johnson, M.; Felix, C. C.; Kampalath, B.; Darkes, M.; Wanggui, Y.; Cameron, B.; Fricker, S. P. *J. Cardiovasc. Pharmacol.* **2002**, *39*, 441.
(7) Yarnell, A. T.; Oh, S.; Reinberg, D.; Lippard, S. J. *J. Biol. Chem.* **2001**, *276*, 25736.
(8) Clarke, M. J.; Zhu, F.; Frasca, D. *Chem. Rev.* **1999**, *99*, 2511.
(9) Antonarakis, E. S.; Emadi, A. *Cancer Chemother. Pharmacol.* **2010**, *66*, 1.
(10) Hartinger, C. G.; Jakupec, M. A.; Seifried, S. Z.; Groessl, M.; Egger, A.; Berger, W.; Zorbas, H.; Dyson, P. J.; Keppler, B. K. *Chem. Biol.* **2008**, *5*, 2140.
(11) Alessio, E.; Mestroni, G.; Bergamo, A.; Sava, G. *Curr. Top. Med. Chem.* **2004**, *4*, 1525.
(12) Bruijnincx, P. C. A.; Sadler, P. J. *Curr. Opin. Chem. Biol.* **2008**, *12*, 197.
(13) (a) Rotzinger, F. P. *Chem. Rev.* **2005**, *105*, 2003 and references therein. (b) Aebischer, N.; Sidorenkova, E.; Ravera, M.; Laurenczy, G.; Osella, D.; Weber, J.; André E. Merbach, A. E. *Inorg. Chem.* **1997**, *36*, 6009.
(14) Richens, D. T. *Chem. Rev.* **2005**, *105*, 1961.
(15) Helm, L.; Merbach, A. E. *Chem. Rev.* **2005**, *105*, 1923.
(16) Erras-Hanauer, H.; Clark, T.; van Eldik, R. *Coord. Chem. Rev.* **2003**, *238*, 233.
(17) Burgess, J.; Hague, D. N.; Kemmitt, R. D. W.; McAuley, A.; Smith, M. A., *Inorganic Reaction Mechanism - A Review of the Literature*; The Chemical Society: London, 1973.
(18) Langford, C. H.; Gray, H. B. *Ligand Substitution Dynamics*; Benjamin: New York, 1965.
(19) Warshel, A.; Levitt, M. *J. Mol. Biol.* **1976**, *103*, 227.
(20) Gao, J. *Rev. Comput. Chem.* **1996**, *7*, 119.
(21) Remsungnen, T.; Rode, B. M. *Chem. Phys. Lett.* **2003**, *367*, 586.
(22) Car, R.; Parrinello, M. *Phys. Rev. Lett.* **1985**, *55*, 2471.
(23) Carloni, P.; Sprik, M.; Andreoni, W. *J. Phys. Chem. B* **2000**, *104*, 823.
(24) Coutinho, K.; Canuto, S. *Adv. Quantum Chem.* **1997**, *28*, 89.
(25) Coutinho, K.; Canuto, S.; Zerner, M. C. *J. Chem. Phys.* **2000**, *112*, 9874.
(26) (a) Spiegel, K.; Magistrato, A. *Org. Biomol. Chem.* **2006**, *4*, 2507 and references therein. (b) Burda, J. V.; Zeizinger, M.; Leszczynski, J. *J. Comput. Chem.* **2005**, *26*, 907. (c) Zhang, Y.; Guo, Z.; You, X. Z. *J. Am. Chem. Soc.* **2001**, *123*, 9378. (d) Robertazzi, A.; Platts, J. A. *J. Biol. Inorg. Chem.* **2005**, *10*, 854. (e) Costa, L. A. S.; Rocha, W. R.; De Almeida, W. B.; Dos Santos, H. F. *Chem. Phys. Lett.* **2004**, *387*, 182and references therein. (f) Costa, L. A. S.; Rocha, W. R.; De Almeida, W. B.; Dos Santos, H. F. *J. Inorg.Biochem.* **2005**, *99*, 575. (g) Carloni, P.; Andreoni, W.; Hutter, J.; Curioni, A.; Giannozzi, P.; Parrinello, M. *Chem. Phys. Lett.* **1995**, *234*, 50. (h) Dorcier, A.; Dyson, P. J.; Gossens, C.; Rothlisberger, U.; Scopelliti, R.; Tavernelli, I. *Organometallics* **2005**, *24*, 2114. (i) Gossens, C.; Tavernelli, I.; Rothlisberger, U. *Chimia* **2005**, *59*, 81. (j) Freccero, M.; Gandolfi, R. *J. Org. Chem.* **2005**, *70*, 7098.
(27) (a) Chen, J.; Chen, L.; Liao, S.; Zheng, K.; Ji, L. *Dalton Trans.* **2007**, 3507. (b) Chen, J.; Chen, L.; Liao, S.; Zheng, K.; Ji, L. *J. Phys. Chem. B* **2007**, *111*, 7862. (c) Bešker, N.; Coletti, C.; Marrone, A.; Re, N. *J. Phys. Chem. B* **2008**, *112*, 3871.
(28) Adamovic, I.; Freitag, M. A.; Gordon, M. S. *J. Chem. Phys.* **2003**, *118*, 6725.
(29) Gordon, M. S.; Freitag, M. A.; Bandyopadhyay, P.; Jensen, J. H.; Kairys, V.; Stevens, W. J. *J. Phys. Chem. A* **2001**, *105*, 293.
(30) Day, P. N.; Jensen, J. H.; Gordon, M. S.; Webb, S. P.; Stevens, W. J.; Krauss, M.; Garmer, D.; Basch, H.; Cohen, D. *J. Chem. Phys.* **1996**, *105*, 1968.
(31) Chen, W.; Gordon, M. S. *J. Chem. Phys.* **1996**, *105*, 11081.
(32) Day, P. N.; Pachter, R.; Gordon, M. S.; Merrill, G. N. *J. Chem. Phys.* **2000**, *112*, 2063.
(33) Adamovic, I.; Gordon, M. S. *J. Phys. Chem. A* **2005**, *109*, 1629.

(34) Slipchenko, L. V.; Gordon, M. S. *J. Phys. Chem. A* **2009**, *113*, 2092.
(35) Yoo, S.; Zahariev, F.; Sok, S.; Gordon, M. S. *J. Chem. Phys.* **2008**, *129*, 144112.
(36) Becke, A. D. *J. Chem. Phys.* **1993**, *98*, 5648.
(37) Lee, C.; Yang, W.; Parr, R. G. *Phys. Rev. B* **1988**, *37*, 785.
(38) Aguilar, C. M.; De Almeida, W. B.; Rocha, W. R. *Chem. Phys. Lett.* **2007**, *449*, 144.
(39) Aguilar, C. M.; De Almeida, W. B.; Rocha, W. R. *Chem. Phys.* **2008**, *353*, 66.
(40) Ferreira, D. E. C.; Florentino, B. P. D.; Nome, F.; Rocha, W. R. *J. Phys. Chem. B* **2009**, *113*, 14831.
(41) Allen, M. P.; Tildesley, D. J. *Computer Simulation of Liquids*; Oxford University Press, Clarendon: New York, 1987.
(42) Metropolis, N.; Rosenbluth, A. W.; Rosenbluth, M. N.; Teller, A. H.; Teller, E. *J. Chem. Phys.* **1953**, *21*, 1087.
(43) Hay, P. J.; Wadt, W. R. *J. Chem. Phys.* **1985**, *82*, 270.
(44) Hehre, W.; Ditchfield, R.; Pople, J. A. *J. Chem. Phys.* **1972**, *56*, 2257.
(45) Breneman, C. M.; Wiberg, K. B. *J. Comput. Chem.* **1990**, *11*, 361.
(46) Jorgensen, W. L.; Madura, J. D.; Swenson, C. J. *J. Am. Chem. Soc.* **1984**, *106*, 6638.
(47) Rappé, A. K.; Casewit, C. J.; Colwell, K. S.; Goddard, W. A., III; Skiff, W. M. *J. Am. Chem. Soc.* **1992**, *114*, 10024.
(48) Jorgensen, W. L.; Chandrasekhar, J.; Madura, J. D.; Impey, R. W.; Klein, M. *J. Chem. Phys.* **1983**, *79*, 926.
(49) Li, Z.; Sheraga, H. A. *Proc. Natl. Acad. Sci. U.S.A.* **1983**, *84*, 6611.
(50) Godbout, N.; Salahub, D. R.; Andzelm, J.; Wimmer, E. *Can. J. Chem.* **1992**, *70*, 560.
(51) Dunning, T. H., Jr. *J. Chem. Phys.* **1989**, *90*, 1007.
(52) Fukui, K. *Acc. Chem. Res.* **1981**, *14*, 363.
(53) Gonzalez, C.; Schlegel, H. B. *J. Chem. Phys.* **1989**, *90*, 2154.
(54) Gonzalez, C.; Schlegel, H. B. *J. Phys. Chem.* **1990**, *94*, 5523.
(55) Møller, C.; Plesset, M. S. *Phys. Rev.* **1934**, *46*, 618.
(56) See, for example: Szabo, A.; Ostlund, N. S. *Modern Quantum Chemistry, Introduction to Advanced Electronic Structure Theory*; Dover Publication, Inc.: New York, 1996.
(57) Woon, D. E.; Dunning, T. H., Jr. *J. Chem. Phys.* **1993**, *98*, 1358.
(58) Kendall, R. A.; Dunning, T. H., Jr. *J. Chem. Phys.* **1992**, *96*, 6796.
(59) Coutinho; K.; Canuto, S. *DICE: A Monte Carlo Program for Liquid Simulation*; University of São Paulo, 1997.
(60) Schmidt, M. W.; Baldridge, K. K.; Boatz, J. A.; Elbert, S. T.; Gordon, M. S.; Jensen, J. H.; Koseki, S.; Matsunaga, N.; Nguyen, K. A.; Su, S. J.; Windus, T. L.; Dupuis, M.; Montgomery, J. A. *J. Comput. Chem.* **1993**, *14*, 1347.
(61) Tomasi, J.; Persico, M. *Chem. Rev.* **1994**, *94*, 2027.
(62) Tomasi, J.; Mennucci, B.; Cammi, R. *Chem. Rev.* **2005**, *105*, 2999.
(63) Pascual-Ahuir, J. L.; Silla, E.; Tomasi, J.; Bonaccorsi, R. *J. Comput. Chem.* **1987**, *8*, 778.
(64) Broomhead, J. A.; Basolo, F.; Pearson, R. G. *Inorg. Chem.* **1964**, *3*, 826.
(65) Eyring, H. *J. Chem. Phys.* **1935**, *3*, 107.
(66) Evans, M. G.; Polanyi, M. *Trans. Faraday Soc.* **1935**, *31*, 875.
(67) Zhao, M.; Clarke, M. J. *J. Biol. Inorg. Chem.* **1999**, *4*, 318.